SCINDEKS
Serbian Citation Index
J Med Biochem 2026; 45 DOI: 10.5937/jomb0-65964

UDK 577.1 : 61 **ISSN 1452-8258**

J Med Biochem 45: 1–9, 2026

Original paper
Originalni naučni rad

PHASE-RELATED CHANGES IN THE SIRTUIN 1–HIGH MOBILITY GROUP BOX 1 AXIS AND NICOTINAMIDE ADENINE DINUCLEOTIDE IN ISCHEMIC STROKE

FAZNO POVEZANE PROMENE U SIRT1–HMGB1 OSI I NIKOTINAMID ADENIN DINUKLEOTIDU KOD ISHEMIJSKOG MOŽDANOG UDARA

Lingling Bai[1], Tao Kang[2]*

[1]Department of Neurological Rehabilitation 6, Xi'an International Medical Centre Hospital, Xian, Shaanxi, 710100, China
[2]Department of Neurology, Xi'an International Medical Centre Hospital, Xian, Shaanxi, 710100, China

Summary

Background: This study investigated phase-related (acute, subacute, and recovery phases) changes in the peripheral blood sirtuin 1 (SIRT1)-high mobility group box 1 (HMGB1) axis after ischemic stroke (IS) and evaluated agreement between enzyme-linked immunosorbent assay and high-performance liquid chromatography for serum nicotinamide adenine dinucleotide (NAD^+) measurement.
Methods: Eighty patients with IS were classified as acute, subacute, or recovery phase according to time from onset, and 40 age- and sex-matched controls were included. Serum SIRT1, HMGB1, acetylated HMGB1, NAD^+, interleukin-1 beta, tumour necrosis factor-alpha, and interleukin-10 were measured. Peripheral blood expression of SIRT1, HMGB1, inducible nitric oxide synthase, and arginase-1 messenger RNA was determined. Agreement for NAD^+ measurement was assessed by Bland-Altman analysis.
Results: In the acute phase, serum SIRT1 and NAD^+ were lowest, whereas HMGB1, acetylated HMGB1, proinflammatory cytokines, and the inducible nitric oxide synthase/arginase-1 ratio were highest ($P<0.05$). Across the subacute and recovery phases, SIRT1 and NAD^+ increased while HMGB1 and Ac-HMGB1 declined, with inflammatory balance indices trending toward control levels. Serum SIRT1 correlated negatively with FMA in the acute phase ($r = -0.737$) and positively in the recovery phase ($r=0.641$). For NAD^+ quantification, ELISA and HPLC

Kratak sadržaj

Uvod: Ova studija je ispitivala fazno zavisne (akutna, subakutna i faza oporavka) promene u osi sirtuin 1 (SIRT1)–proteina visoke mobilnosti grupe B1 (HMGB1) u perifernoj krvi nakon ishemijskog moždanog udara (IMU), kao i saglasnost između enzimski povezanog imunosorbentnog testa (ELISA) i tečne hromatografije visokih performansi (HPLC) za određivanje serumskog nikotinamid adenin dinukleotida (NAD^+).
Metode: U studiju je uključeno 80 pacijenata sa IMU, koji su svrstani u akutnu, subakutnu ili fazu oporavka prema vremenu proteklom od nastanka simptoma, kao i 40 zdravih ispitanika usklađenih po uzrastu i polu. Mereni su serumski nivoi SIRT1, HMGB1, acetilisanog HMGB1, NAD^+, interleukina-1β, faktora tumorske nekroze alfa i interleukina-10. Određena je i ekspresija mRNK SIRT1, HMGB1, inducibilne azot-monoksid sintaze i arginaze-1 u perifernoj krvi. Saglasnost između ELISA i HPLC metoda za određivanje NAD^+ procenjena je Bland-Altman analizom.
Rezultati: U akutnoj fazi, serumski nivoi SIRT1 i NAD^+ bili su najniži, dok su HMGB1, acetilisani HMGB1, proinflamatorni citokini i odnos inducibilne azot-monoksid sintaze i arginaze-1 bili najviši ($P<0,05$). Tokom subakutne faze i faze oporavka, SIRT1 i NAD^+ su se postepeno povećavali, dok su HMGB1 i Ac-HMGB1 opadali, uz približavanje pokazatelja inflamatorne ravnoteže kontrolnim vrednostima. Serumski SIRT1 je u akutnoj fazi negativno korelirao

Address for correspondence:

Tao Kang
Department of Neurology, Xi'an International Medical Centre Hospital
Xian, Shaanxi, 710100, China
e-mail: kangtao0709@163.com

demonstrated generally good agreement, with approximately 90% agreement in IS samples.
Conclusion: Peripheral blood indices related to the SIRT1-HMGB1 axis show phase-dependent changes after IS and are accompanied by parallel changes in inflammatory status and motor function. Enzyme-linked immunosorbent assay showed acceptable agreement with high-performance liquid chromatography for serum NAD^+ measurement.

Keywords: biomarkers, HMGB1 protein, ischemic stroke, NAD^+, Sirtuin 1, recovery phase

sa FMA skorom (r=-0,737), a u fazi oporavka pozitivno (r=0,641). Za kvantifikaciju NAD^+, ELISA i HPLC pokazale su dobru saglasnost, sa približno 90% podudarnosti u uzorcima pacijenata sa IMU.
Zaključak: Periferni krvni indeksi koji su povezani sa osom SIRT1–HMGB1 pokazuju fazno zavisne promene nakon ishemijskog moždanog udara, praćene paralelnim promenama u inflamatornom statusu i motoričkoj funkciji. ELISA metoda pokazuje prihvatljivu saglasnost sa HPLC za merenje serumskog NAD^+.

Ključne reči: biomarkeri, HMGB1 protein, ishemijski moždani udar, NAD^+, sirtuin 1, faza oporavka

Introduction

High mobility group box 1 (HMGB1), a prototypical damage-associated molecular pattern, is released from injured neurons and glia under ischemic and hypoxic stress. Once extracellular, HMGB1 can engage inflammatory signalling pathways such as TLR4/NF-κB, amplifying microglial activation and the production of mediators including IL-1β and TNF-α, thereby aggravating secondary injury and worsening motor outcomes (1, 2). In contrast, sirtuin 1 (SIRT1), an NAD^+-dependent deacetylase, is widely regarded as a neuroprotective regulator in cerebral ischemic injury; via deacetylation of downstream substrates, it can temper oxidative stress and inflammatory signalling (3, 4). Although the SIRT1–HMGB1 axis has been implicated in several inflammation-related conditions, its phase-dependent biochemical behaviour after ischemic stroke (IS) – particularly in relation to recovery – has not been well characterized (5). The study by Yao W et al. (6), showed that SIRT1 can deacetylate key lysine residues on HMGB1, thereby restricting its nucleocytoplasmic translocation and limiting extracellular release, thereby dampening downstream inflammatory signalling. Clinically, higher circulating HMGB1 levels have been associated with more severe neurological deficits in IS, while pharmacological activation of SIRT1 has been linked to reduced tissue injury through improved microcirculation and inhibition of maladaptive glial responses (7). However, much of the available work has evaluated SIRT1 or HMGB1 in isolation. A coherent, cross-sectional view of how the combined axis behaves across the trajectory from inflammatory initiation to resolution and repair after IS – and how that trajectory aligns with motor recovery – remains limited.

Against this background, the present study focused on the regulatory network cantered on the deacetylation of the SIRT1–HMGB1 axis. We tracked its laboratory profile across the acute, subacute, and recovery phases of IS. We examined whether changes in this axis were aligned with markers of polarization balance (iNOS and Arg-1) and with motor function, as captured by the FMA (8).

Materials and Methods

Sample source

Eighty patients with IS treated at our hospital's Department of Neurology between January 2024 and December 2024 were enrolled as the case cohort. During the same period, 40 individuals undergoing routine physical examination were recruited as healthy controls.

Sample size calculation

Sample size was estimated using serum HMGB1 as the primary variable, assuming an expected difference of approximately 3.2 ng/mL between healthy individuals and acute-phase IS patients/mL based on previous literature (8) and preliminary experiments, with an SD of 1.5 ng/mL. Using PASS 15.0 with a two-sided $\alpha=0.05$ and $\beta=0.2$ (80% power) and an effect size $d=0.8$, the minimum required size was 23 participants per group. To accommodate loss to follow-up and analytical variability, each IS-phase subgroup was expanded to 25–28 cases (total n=80), and the control group was set to 40 participants (50% of the case cohort) to maintain adequate power for intergroup comparisons.

Inclusion and exclusion criteria

Exclusion criteria: ① Haemorrhagic stroke or mixed stroke; ② A history of major neurological disorders (e.g., Parkinson's disease, Alzheimer's disease); ③ Recent use of immunosuppressants, anti-inflammatory agents, or medications known to affect SIRT1 activity; ④ Incomplete clinical data.

Inclusion criteria (control group): Age- and sex-matched to the case cohort, no history of cerebrovascular disease or other severe organic disease, and no recent use of medications that materially influence inflammatory responses or SIRT1 activity.

Grouping design

Participants were allocated to four groups: healthy controls (n=40), IS acute phase (onset ≤7 days, n=27), IS subacute phase (onset 8–14 days, n=28), and IS recovery phase (onset 15–90 days, n=25). The time window criteria for IS staging were adopted from previous clinical studies of ischemic stroke (9). Peripheral blood was collected from Participants. This study was conducted in full accordance with the ethical principles of the Declaration of Helsinki and its later amendments. The Ethics Committee of Xi'an International Medical Centre Hospital approved the study protocol. Written informed consent was obtained from all participants in both the case and control groups before enrolment.

Main reagents and instruments

Human SIRT1, HMGB1, and acetylated HMGB1 (Ac-Lys29) ELISA kits (Yilei Te Biotechnology Co., Ltd., Wuhan; Huamei Biotechnology Co., Ltd., Wuhan); human IL-1β, TNF-α, and IL-10 ELISA kits (Boster Biological Technology Co., Ltd., Wuhan); human NAD^+ ELISA kit (Jiancheng Bioengineering Institute, Nanjing); Trizol reagent, reverse transcription kit, and qPCR kit (Invitrogen; TaKaRa); RNA extraction kit (Tiangen Biochemical Technology Co., Ltd., Beijing). StepOnePlus™ Real-Time PCR System (Thermo Fisher); Multiskan FC Microplate Reader (Thermo Fisher); Agilent 1260 HPLC System (Agilent Technologies); Centrifuge 5810R refrigerated centrifuge (Eppendorf); DW-86L626 ultra-low temperature freezer (Haier Biomedical); NanoDrop 2000 spectrophotometer (Thermo Fisher). The intra-assay coefficient of variation (CV) for all ELISA kits was <5%, and the inter-assay CV was <8%, both within kit quality control specifications.

Sample processing and detection methods

Peripheral blood sample processing

Fasting venous blood (8 mL) was collected from each participant in the early morning. Four millilitres were placed into a serum tube, allowed to clot at room temperature for 30 min, and centrifuged at 3000 rpm for 15 min. Serum was aliquoted and stored at -80 °C for ELISA and HPLC. The remaining 4 mL were collected into an EDTA tube, gently inverted to mix, and centrifuged at 3000 rpm for 10 min to obtain plasma for total RNA extraction. Extracted RNA was either reverse-transcribed immediately or stored at -80 °C until use.

ELISA

Assays were performed according to the manufacturers' protocols to measure serum SIRT1, HMGB1, Ac-HMGB1, IL-1β, TNF-α, IL-10, and NAD^+.

qPCR detection

Total RNA was extracted from plasma using Trizol. RNA purity and concentration were assessed by spectrophotometry, and cDNA was generated by reverse transcription. qPCR was run with GAPDH as the reference gene. Relative mRNA expression of SIRT1, HMGB1, iNOS, and Arg-1 was calculated using the $2^{-\Delta\Delta Ct}$ method. Cycling conditions were: 95 °C for 30 s; 40 cycles of 95 °C for 5 s and 60 °C for 30 s. The primer sequences were designed and constructed by Suzhou Synda Gene Technology Co., LTD (*Table I*).

HPLC

Serum NAD^+ was quantified by HPLC using a C18 column. The mobile phase consisted of methanol and 0.05 mol/L potassium dihydrogen phosphate buffer; flow rate, 1.0 mL/min; detection wavelength, 260 nm; column temperature, 30 °C; injection volume, 20 μL. Samples were protein-precipitated with methanol at a ratio of methanol:serum = 3:1, vortexed, incubated on ice for 10 min, centrifuged, filtered, and injected. Peaks were identified by retention time against an NAD^+ standard and quantified by peak area to verify the ELISA results. Method validation for HPLC detection of serum NAD^+ was performed. The linear range was 0.5–50.0 μmol/L (R^2=0.998). The limit of

Table I Primer sequences.

Gene	F (5′→3′)	R (5′→3′)	bp
GAPDH	GGAGCGAGATCCCTCCAAAAT	GGCTGTTGTCATACTTCTCATGG	197
SIRT1	GGCAGAAATGGCAAAGTGGAC	TCTCGGAGCTGCTATGTCTGT	156
HMGB1	AGCCTCAAAAGGAAGACGAGG	GGATGGCCTTCTTCTGCTTG	142
iNOS (NOS2)	CCCTTCCGAAGTTTCTGGCAGC	GGCTGTCAGAGCCTCGTGGCT	189
Arginase-1 (ARG1)	CAGACCAGGGTCCTGGACAA	TCACAGTCTTCCCAAGCTGGT	163

detection (LOD) was 0.12 μmol/L, and the limit of quantification (LOQ) was 0.36 μmol/L. Intra-day precision was < 3%, inter-day precision was < 5%, and the sample recovery rate was 92.6%–105.3%.

Agreement analysis between ELISA and HPLC for serum NAD$^+$

The agreement between ELISA and HPLC for serum NAD$^+$ measurement was evaluated in paired serum samples. Bland-Altman analysis was used to assess consistency, with the agreement range defined as ±1.96 SD of the mean difference. The proportion of paired results within this range was defined as the agreement rate. HPLC was used as the comparative method for laboratory evaluation of ELISA-derived NAD$^+$ results.

Laboratory quality control

Serum and plasma samples were subjected to no more than 2 freeze-thaw cycles. Laboratory personnel performing ELISA and HPLC were blinded to group assignment. All assays were performed according to the manufacturer's instructions and standard operating procedures. Samples were processed under the same pre-analytical conditions and analysed using a uniform workflow. Quality control materials (lot numbers: QC-SIRT-001, QC-HMGB-002) were included in each analytical run, and deviations within ±10% of the target value were considered acceptable; samples with obvious haemolysis, lipemia, or clotting were excluded.

Motor function assessment

Motor function was assessed at onset (≤7 days; acute), 8–14 days (subacute), and 15–90 days (recovery) by two trained neurologists blinded to group assignment using the Fugl–Meyer Assessment (FMA), a 100-point scale of motor function (10). The FMA covers six domains (including upper limb, lower limb, and balance), with a maximum score of 100; higher scores indicate better motor performance. The mean of the two ratings was used for analysis.

Statistical analysis

SPSS 26.0 was used for statistical analyses. Continuous variables are presented as mean ± standard deviation, and one-way analysis of variance (ANOVA) was used for intergroup comparisons, with LSD-t tests for post hoc pairwise comparisons. Categorical variables are presented as n (%), and the χ^2 test was applied for group comparisons. Normality was tested using the Shapiro-Wilk test. Pearson correlation was used for normally distributed data, and Spearman correlation for non-normally distributed data. Confounding factors (hypertension, diabetes, hyperlipidaemia, and coronary heart disease) were adjusted by analysis of covariance (ANCOVA) in group comparisons and by partial correlation in SIRT1–FMA correlation analysis. The agreement between ELISA and HPLC for NAD$^+$ quantification was evaluated using Bland-Altman analysis. A two-sided $P<0.05$ was considered statistically significant.

Results

Summary

Collectively, changes in the SIRT1-HMGB1 axis were consistent with parallel shifts in inflammatory factor levels and the iNOS/Arg-1 ratio across acute, subacute, and recovery phases after IS.

Analysis of baseline comparability

Baseline characteristics were comparable across groups for sex, age, and BMI ($P>0.05$) (*Table II*).

Comparison of Serum SIRT1 and HMGB1

Serum SIRT1 concentrations differed among groups ($P<0.05$). Controls showed the highest SIRT1 levels, whereas acute-phase patients had the lowest. SIRT1 increased progressively during the subacute and recovery phases, and values in the recovery phase were not significantly different from those in controls ($P>0.05$). Serum HMGB1 and Ac-HMGB1 showed an inverse pattern relative to SIRT1 ($P<0.05$). Both markers peaked in the acute phase: HMGB1 increased by more than threefold and Ac-HMGB1 by more than sixfold compared with controls. Concentrations declined in the subacute and recovery phases, and HMGB1 in the recovery phase approximated control values ($P>0.05$). The Ac-HMGB1/HMGB1 ratio was highest in the acute phase (0.53±0.17) and remained higher in the recovery phase than in controls ($P<0.05$). Relative mRNA expression of SIRT1 and HMGB1 in peripheral blood differed among groups ($P<0.05$) and mirrored the serum protein patterns. SIRT1 mRNA was lowest in the acute phase and rose across phases; in the recovery phase, it reached 0.83±0.11 and did not differ significantly from controls ($P>0.05$). HMGB1 mRNA was highest in the acute phase (3.33±0.053) and decreased toward control levels by the recovery phase ($P>0.05$) (*Figure 1*).

Table II Comparison of baseline clinical data among all groups.

	Control Group	Acute Phase	Subacute Phase	Recovery Phase	χ^2 (or t)	P
	n=40	n=27	n=28	n=25		
Sex					0.081	0.994
Male	23 (57.5)	16 (59.3)	17 (60.7)	15 (60.0)		
Female	17 (42.5)	11 (40.7)	11 (39.3)	10 (40.0)		
Age	61.9±6.2	64.6±8.6	60.6±8.3	61.8±8.4	1.183	0.319
BMI	23.2±2.1	23.6±1.5	23.1±1.9	23.4±2.3	0.296	0.828
History of Hypertension	8 (20.0)	21 (77.8)	22 (78.6)	20 (80.0)	38.122	<0.001
History of Diabetes	6 (15.0)	15 (55.6)	16 (57.1)	14 (56.0)	18.583	<0.001
History of Hyperlipidaemia	7 (17.5)	18 (66.7)	19 (67.9)	17 (68.0)	26.694	<0.001
History of Coronary Heart Disease	4 (10.0)	10 (37.0)	11 (39.3)	9 (36.0)	10.012	0.019
Smoking					4.123	0.249
Yes	7 (17.5)	10 (37.0)	10 (35.7)	8 (32.0)		
No	33 (82.5)	17 (63.0)	18 (64.3)	17 (68.0)		
Infarct Site					1.357	0.968
Middle Cerebral Artery	-	19 (70.4)	20 (71.4)	18 (72.0)		
Lobar Area	-	4 (14.8)	4 (14.3)	3 (12.0)		
Vertebrobasilar Artery Area	-	3 (11.1)	3 (10.7)	4 (16.0)		
Multifocal	-	1 (3.7)	1 (3.6)	0 (0.0)		

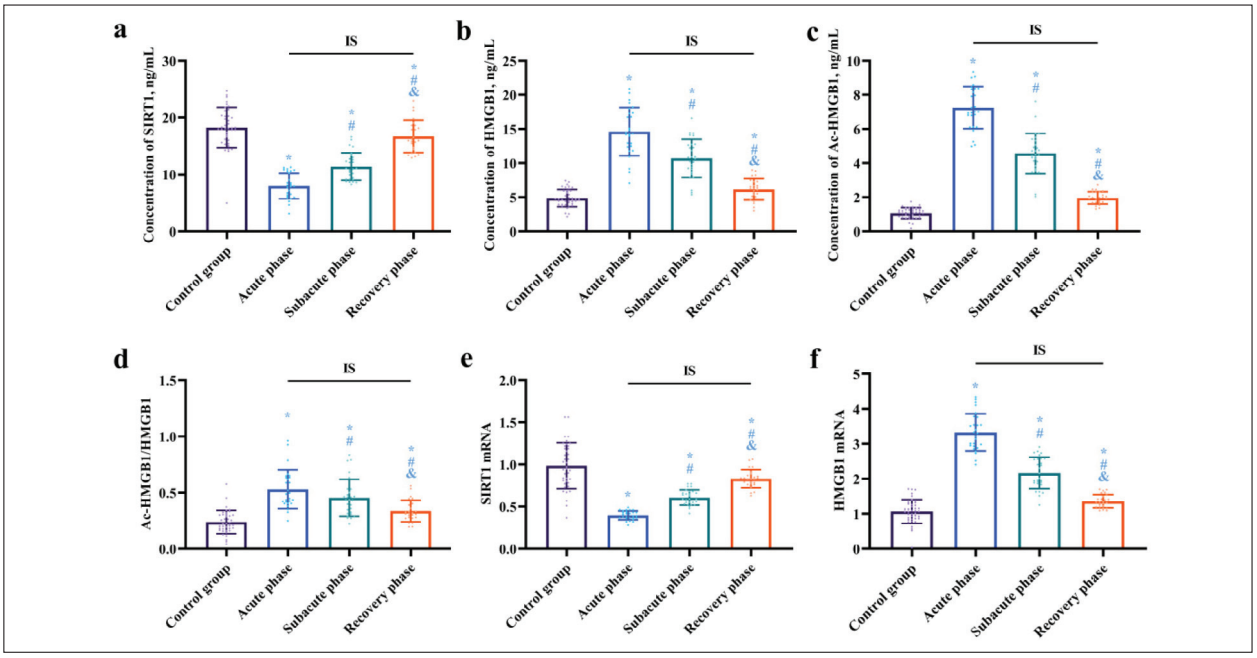

Figure 1 Comparisons of Serum SIRT1 and HMGB1.

(a) Serum SIRT1 concentration; (b) Serum HMGB1 concentration; (c) Serum Ac-HMGB1 concentration; (d) Serum Ac-HMGB1/HMGB1 ratio; (e) Relative mRNA expression level of SIRT1; (f) Relative mRNA expression level of HMGB1. n=40 (control), 27 (acute), 28 (subacute), 25 (recovery). *P<0.05 vs. control group, #P<0.05 vs. acute phase, &P<0.05 vs. subacute phase.

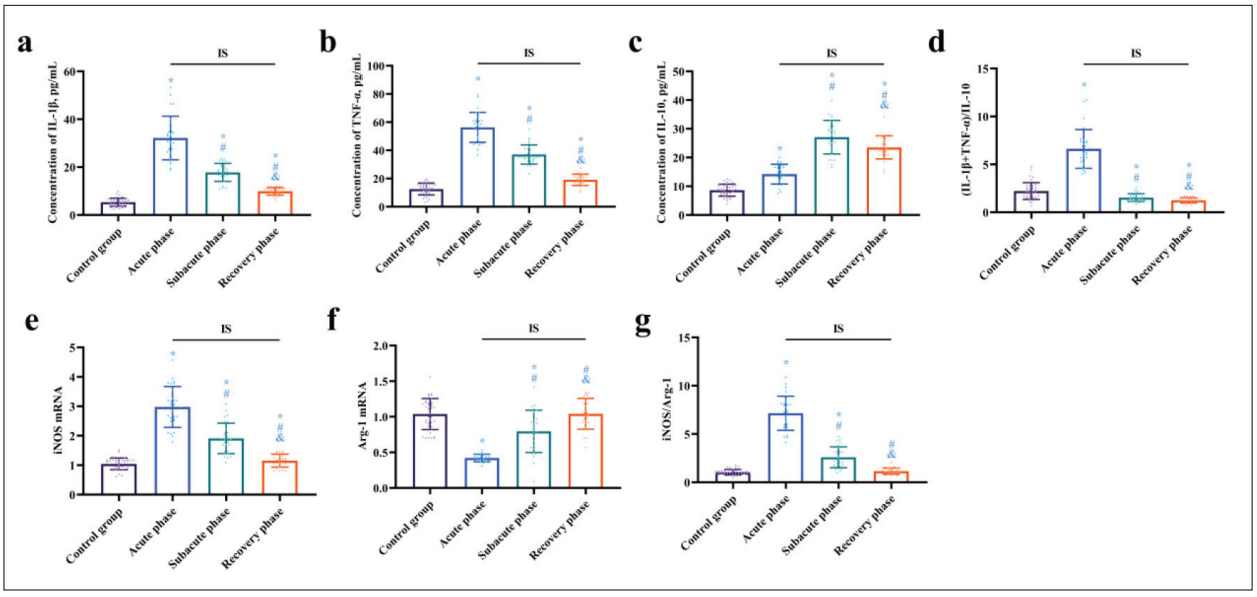

Figure 2 Comparisons of Inflammatory Factor and iNOS/Arg-1.

(a) Serum IL-1β concentration; (b) Serum TNF-α concentration; (c) Serum IL-10 concentration; (d) (IL-1β + TNF-α)/IL-10 ratio; (e) Relative mRNA expression level of iNOS; (f) Relative mRNA expression level of Arg-1; (g) iNOS/Arg-1 ratio. n=40 (control), 27 (acute), 28 (subacute), 25 (recovery). *P<0.05 vs. control group, #P<0.05 vs. acute phase, & P<0.05 vs. subacute phase.

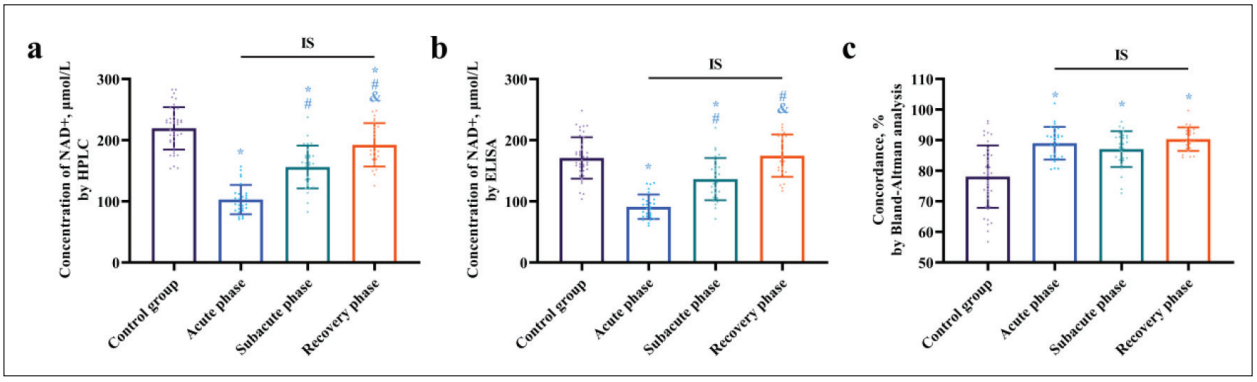

Figure 3 Serum NAD^+ concentrations measured by ELISA and HPLC, and consistency analysis among groups.

(a) Serum NAD^+ concentration detected by HPLC; (b) Serum NAD^+ concentration detected by ELISA; (c) Bland-Altman consistency analysis of NAD^+ detection results. n=40 (control), 27 (acute), 28 (subacute), 25 (recovery). *P<0.05 vs. control group, #P<0.05 vs. acute phase, &P<0.05 vs. subacute phase.

Comparison of Serum Inflammatory Factor and iNOS/Arg-1

Serum IL-1β and TNF-α concentrations differed among groups (P<0.05). Both were markedly elevated in the acute phase, rising by more than sixfold and fivefold, respectively, relative to controls. Levels declined during the subacute phase and did not differ significantly between the recovery phase and controls (P>0.05). IL-10 exhibited an opposing pattern (P<0.05), with a modest increase in the acute phase and peaking at (27.10±5.84) pg/mL in the subacute phase. Although IL-10 decreased in the recovery phase, it remained higher than in controls (P<0.05). Consistently, the (IL-1β+TNF-α)/IL-10 ratio was highest in the acute phase, fell sharply in the subacute and recovery phases, and was lower than in controls (P<0.05). Secondly, in the acute phase, iNOS mRNA expression was highest and Arg-1 expression lowest, yielding a peak iNOS/Arg-1 ratio (7.15±1.77). In the subacute phase, iNOS decreased while Arg-1 increased, resulting in a declining ratio. In the recovery phase, Arg-1 expression approached control values (P>0.05), consistent with a shift toward restoration of polarization balance (*Figure 2*).

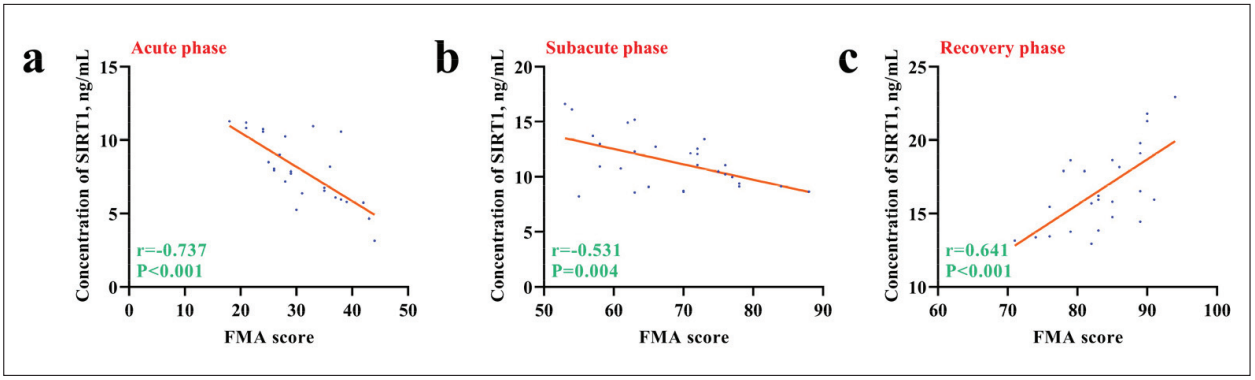

Figure 4 Correlation analyses between Serum SIRT1 concentration and FMA Score.

(a) Correlation in acute phase; (b) Correlation in subacute phase; (c) Correlation in recovery phase. Correlation analysis between serum SIRT1 concentration and FMA score in each phase; $P<0.05$ for significant correlations.

Analysis of serum NAD⁺ concentration and detection consistency

Both HPLC and ELISA showed a concordant phase-dependent pattern of serum NAD^+ in IS. The healthy control group exhibited the highest NAD^+ concentration, which fell markedly in the acute phase and then increased progressively through the subacute and recovery phases. Notably, NAD^+ levels in the recovery phase did not differ significantly from those in controls ($P>0.05$). Method comparison indicated generally good agreement between ELISA and HPLC for NAD^+ quantification. Based on the Bland-Altman consistency analysis, agreement in IS samples was approximately 90%, supporting the practical use of ELISA for batch testing, whereas agreement in the control group was comparatively lower (78.07±10.21%) (*Figure 3*).

Correlation between Serum SIRT1 and FMA Score

The FMA score was lowest in the acute phase group (30.816±7.14 points), indicating severe motor dysfunction. Scores increased in the subacute phase and further rose to 83.56±5.87 points in the recovery phase group, suggesting marked motor improvement. The healthy control group had no relevant scores and was not included in the comparison. Correlation analysis showed a significant association between serum SIRT1 concentration and FMA score ($P<0.05$): a negative correlation was observed in the acute phase group ($r=-0.737$), whereas a positive correlation was found in the recovery phase group ($r=0.641$) (*Figure 4*).

Discussion

The present study showed clear phase-related changes in peripheral blood laboratory indices after IS (11). In the acute phase, serum SIRT1 and NAD^+ were reduced, whereas HMGB1, Ac-HMGB1, IL-1β, and TNF-α were increased. During the subacute and recovery phases, SIRT1 and NAD^+ differed significantly across phases, while HMGB1 and Ac-HMGB1 declined.

An important finding of this study was the opposite pattern observed for SIRT1/NAD^+ and HMGB1/Ac-HMGB1. Because SIRT1 is NAD^+ dependent, its activity is closely coupled to NAD^+ availability (12). Here, serum NAD^+ decreased significantly in acute-phase IS and followed the same direction of change as serum SIRT1, which is consistent with the view that NAD^+ depletion may constrain SIRT1 deacetylation capacity early after injury (13). Concurrently, serum HMGB1 and its acetylated form (Ac-HMGB1) increased sharply, and the Ac-HMGB1/HMGB1 ratio peaked while SIRT1 reached its nadir, consistent with a negative regulatory relationship between SIRT1 and HMGB1 acetylation. Mechanistically, these data suggest that SIRT1 may deacetylate HMGB1 lysine residues (e.g., Lys29), limiting nucleocytoplasmic translocation and extracellular release (14). When SIRT1 activity is insufficient, HMGB1 acetylation and release increase, and downstream pathways, such as TLR4/NF-κB, are activated, promoting a surge of proinflammatory mediators (15). In our data, IL-1β and TNF-α were elevated in the acute phase and changed in parallel with Ac-HMGB1, consistent with prior mechanistic reports (16). Importantly, these relationships were captured in a clinical sample setting rather than an experimental model.

Inflammation resolution represents an active process that shapes tissue repair after IS (17). By combining serum mediator profiling with polarization-related transcripts, our data suggest that the SIRT1–HMGB1 axis is aligned with the balance between iNOS (M1-leaning) and Arg-1 (M2-leaning) signals (18). In a study by Zhao X et al. on articular

chondrocytes, they found that acetylated HMGB1 amplifies NF-κB activity, promoting iNOS transcription and M1 polarization (19), whereas restoration of SIRT1 activity reduces HMGB1 acetylation and restrains inflammatory signalling, permitting Arg-1-associated, M2-leaning programs to dominate (20). These previous studies may explain the current study's findings. However, this study did not conduct mechanistic verification at the cellular level, and the above inferences regarding the association between the SIRT1-HMGB1 axis and microglial polarization still need to be further confirmed by subsequent basic experiments.

In this cohort, improvement in the laboratory profile – higher NAD^+/SIR–T1, lower HMGB1 and Ac-HMGB1, and a more favourable pro-to-anti-inflammatory balance – occurred alongside rising FMA scores. In the study by Zhang W et al. (21), resolution of inflammation reduces ongoing injury to neurons and synapses, creating conditions more permissive for remodelling. In addition, anti-inflammatory mediators such as IL-10, often associated with M2-leaning states, may support repair pathways by favouring trophic signalling and the reconstruction of disrupted circuits (22). The persistently higher IL-10 in the later phases, together with improved FMA scores, is consistent with this interpretation.

Finally, ELISA and HPLC showed a similar phase-dependent pattern for serum NAD^+, and Bland-Altman analysis indicated generally good agreement in IS samples. This finding supports the practical value of ELISA for higher-throughput measurement of serum NAD^+ in this setting. However, the lower agreement observed in controls indicates that matrix effects or a narrow concentration range may influence consistency between methods.

This study had several limitations. First, the case group had a significantly higher prevalence of hypertension, diabetes, hyperlipidaemia, and coronary heart disease than the control group, which may exert confounding effects on the results. Second, this cross-sectional design lacked longitudinal follow-up of the same individuals, so intra-individual dynamic changes in the SIRT1-HMGB1 axis could not be clarified. Third, this was a single-centre study with a modest sample size, and causal inference was not possible. Fourth, HMGB1 acetylation was evaluated by targeted ELISA rather than site-specific structural analysis.

Conclusion

Peripheral blood SIRT1, HMGB1, Ac-HMGB1, NAD^+, and inflammation-related indices showed phase-dependent changes after IS. Differences in FMA scores across disease phases accompanied these laboratory changes. The findings suggest a correlation of the SIRT1–HMGB1 axis with post-stroke inflammatory status and motor recovery. ELISA and HPLC showed generally good agreement for serum NAD^+ measurement in IS samples. The phase-dependent changes in the SIRT1-HMGB1 axis identified in this study may provide potential peripheral blood biomarkers for evaluating the inflammatory state, disease course, and prognosis in patients with ischemic stroke.

Consent to publish

All authors gave final approval of the version to be published.

Availability of data and materials

The data used to support the findings of this study are available from the corresponding author upon request.

Funding

None.

Conflict of interest statement

All the authors declare that they have no conflict of interest in this work.

References

1. Gao B, Wang S, Li J, Han N, Ge H, Zhang G, et al. HMGB1, angel or devil, in ischemic stroke. Brain Behav 2023; 13(5): e2987.
2. Li J, Wang Z, Li J, Zhao H, Ma Q. HMGB1: A New Target for Ischemic Stroke and Hemorrhagic Transformation. Transl Stroke Res 2025; 16(3): 990–1015.
3. Jia Z, Xu K, Li R, Yang S, Chen L, Zhang Q, et al. The critical role of Sirt1 in ischemic stroke. Front Pharmacol 2025; 16: 1425560.
4. Tang H, Wen J, Qin T, Chen Y, Huang J, Yang Q, et al. New insights into Sirt1: potential therapeutic targets for the treatment of cerebral ischemic stroke. Front Cell Neurosci 2023; 17: 1228761.
5. Wei L, Zhang W, Li Y, Zhai J. The SIRT1-HMGB1 axis: Therapeutic potential to ameliorate inflammatory responses and tumor occurrence. Front Cell Dev Biol 2022; 10: 986511.
6. Yao W, Tao R, Wang K, Ding X. Icariin attenuates vascular endothelial dysfunction by inhibiting inflammation through GPER/Sirt1/HMGB1 signaling pathway in type 1 diabetic rats. Chin J Nat Med 2024; 22(4): 293–306.
7. Du O, Yan YL, Yang HY, Yang YX, Wu AG, Guo YK, et al. ALPK1 signaling pathway activation by HMGB1 drives microglial pyroptosis and ferroptosis and brain injury after acute ischemic stroke. Int Immunopharmacol 2025; 149: 114229.
8. Fan J, He K, Zhang Y, Li R, Yi X, Li S. HMGB1: new biomarker and therapeutic target of autoimmune and autoinflammatory skin diseases. Frontiers in immunology 2025; 16: 1569632.
9. Huang YT, Tang CC, Chung CC, Chung CH. Effects of oral care combined with neuromuscular electrical stimulation on clinical outcomes in the acute phase of acute ischemic stroke: a pilot randomized controlled trial. J Neuroeng Rehabil 2025; 22(1): 122.
10. de Blas-Zamorano P, Montagut-Martinez P, Perez-Cruzado D, Merchan-Baeza JA. Fugl-Meyer Assessment for upper extremity in stroke: A pyschometric systematic review. J Hand Ther 2025; 39(1): 22–51.
11. Patabendige A, Singh A, Jenkins S, Sen J, Chen R. Astrocyte Activation in Neurovascular Damage and Repair Following Ischaemic Stroke. Int J Mol Sci 2021; 22(8): 4280.
12. Chen L, Chen S, Bai Y, Zhang Y, Li X, Wang Y, et al. Electroacupuncture improves cognitive impairment after ischemic stroke based on regulation of mitochondrial dynamics through SIRT1/PGC-1alpha pathway. Brain Res 2024; 1844: 149139.
13. Ou Z, Zhao M, Xu Y, Wu Y, Qin L, Fang L, et al. Huangqi Guizhi Wuwu decoction promotes M2 microglia polarization and synaptic plasticity via Sirt1/NF-kappaB/NLRP3 pathway in MCAO rats. Aging 2023; 15(19): 10031–56.
14. Zhang X, Zhang F, Yao F, Wang P, Xiong Q, Neng P. Bergenin has neuroprotective effects in mice with ischemic stroke through antioxidative stress and anti-inflammation via regulating Sirt1/FOXO3a/NF-kappaB signaling. Neuroreport 2022; 33(13): 549–60.
15. Zhao PC, Xu SN, Huang ZS, Jiang GW, Deng PC, Zhang YM. Hyperbaric oxygen via mediating SIRT1-induced deacetylation of HMGB1 improved cReperfusion inj/reperfusion injury. Eur J Neurosci 2021; 54(9): 7318–31.
16. Bian H, Xiao L, Liang L, Xie Y, Wang H, Slevin M, et al. Polydatin Prevents Neuroinflammation and Relieves Depression via Regulating Sirt1/HMGB1/NF-kappaB Signaling in Mice. Neurotox Res 2022; 40(5): 1393–404.
17. Alsbrook DL, Di Napoli M, Bhatia K, Biller J, Andalib S, Hinduja A, et al. Neuroinflammation in Acute Ischemic and Hemorrhagic Stroke. Current neurology and neuroscience reports 2023; 23(8): 407–31.
18. Zhou S, Yang X, Mo K, Ning Z. Pyroptosis and polarization of macrophages in septic acute lung injury induced by lipopolysaccharide in mice. Immun Inflamm Dis 2024; 12(3): e1197.
19. Zhao X, Li M, Lu Y, Wang M, Xiao J, Xie Q, et al. Sirt1 inhibits macrophage polarization and inflammation in gouty arthritis by inhibiting the MAPK/NF-kappaB/AP-1 pathway and activating the Nrf2/HO-1 pathway. Inflamm Res 2024; 73(7): 1173–84.
20. Li J, Yu M, Zong R, Fan C, Ren F, Wu W, et al. Deacetylation of Notch1 by SIRT1 contributes to HBsAg- and HBeAg-mediated M2 macrophage polarization. Am J Physiol Gastrointest Liver Physiol 2022; 322(4): G459–G71.
21. Zhang W, Xiao D, Mao Q, Xia H. Role of neuroinflammation in neurodegeneration development. Signal Transduct Target Ther 2023; 8(1): 267.
22. Liu B, Zhang Y, Yang Z, Liu M, Zhang C, Zhao Y, et al. Omega-3 DPA Protected Neurons from Neuroinflammation by Balancing Microglia M1/M2 Polarizations through Inhibiting NF-kappaB/MAPK p38 Signaling and Activating Neuron-BDNF-PI3K/AKT Pathways. Mar Drugs 2021; 19(11): 587.

Recieved: March 20; 2026
Accepted: April 17, 2026